



# Adaptive nonsingular fixed-time sliding mode control for manipulator systems' trajectory tracking

Xin Zhang<sup>1,2</sup> · Ran Shi<sup>1</sup> · Zijun Zhu<sup>1</sup> · Ying Quan<sup>1</sup>

Received: 19 May 2022 / Accepted: 27 August 2022 / Published online: 23 September 2022  
© The Author(s) 2022

## Abstract

In this paper, an adaptive fixed-time controller is raised for the manipulator system with uncertain disturbances to boost the rate and precision of its trajectory tracking and solve the convergence time dependence on the system's initial conditions. First, a nonsingular fixed-time sliding mode (SM) surface and a reaching law based on an arctangent function are constructed to enhance the control scheme performance. Second, the upper bound is difficult to obtain because of the uncertainty of the disturbance. The disturbance upper bound is estimated by adaptive techniques, which do not require a priori knowledge about the upper bound and effectively inhibit the effect of disturbance on the system. Finally, the fixed-time convergence of the states is analyzed by rigorous theoretical proof, and the validity of the presented control scheme is demonstrated by simulation.

**Keywords** Nonsingular fixed-time sliding mode (SM) surface · Adaptive techniques · Disturbance upper bound · Manipulator system

## Introduction

As robotics advances, manipulator schemes are being fully utilized as the core part of robots to replace humans in complex, repetitive, and dangerous tasks. The manipulator scheme's high-precision trajectory tracking is indispensable for all of the above tasks. The robotic manipulator is a time-varying nonlinear system with external disturbances and parameter uncertainty effects. Thus, for nonlinear system control issues, sliding mode control (SMC) [1–6], neural network control [7–9], fuzzy control [10–14], and adaptive control [15, 16] have been used. Among them, SMC has the advantages of fast dynamic response, excellent robustness, and relatively simple control implementation.

The common SMC uses a linear SM surface, and [17] designed an SMC based on a super-twisting method for the robotic manipulator system control issue, considering that it uses a linear SM surface and does not have finite-time convergence capability, and the linear error SM surface has slow convergence and large chattering problems. The ordinary linear SM surface can only approach the equilibrium point in infinite time. To obtain better performance, finite-time SMC has been fully developed. In [18], a nonsingular terminal sliding mode (TSM) controller is presented for the magnetic levitation scheme control issue, achieving finite-time control of the error states and effectively addressing the singularity issue. By bringing in a new error term, a nonsingular fast TSM surface is proposed for the first time in [19], which achieves a fast convergence of the full phase of the error while increasing the control accuracy. In [20], a nonsingular fast TSM controller is proposed to effectively improve the underwater vehicle control issue by estimating the disturbance magnitude through a state observer. Nonsingular fast TSM surfaces have been fully utilized in different systems [21–23]. To eliminate the singularity, an adjustment of the reaching law is required under the action of the nonsingular fast TSM surface, which may affect the rate of convergence of the error states. In [24, 25], nonsingular fast TSM surfaces based on piecewise functions were proposed, which effectively solved the problems of nonsingular fast TSM surfaces

✉ Ran Shi  
12201420@stu.lzjtu.edu.cn

<sup>1</sup> School of Automation and Electrical Engineering, Lanzhou Jiaotong University, Lanzhou 730070, China

<sup>2</sup> Gansu Provincial Engineering Research Center for Artificial Intelligence and Graphics and Image Processing, Lanzhou 730070, China

while avoiding the singularity issue. However, the convergence time of the system state in the above literature depends on the initial conditions, which means that the convergence time is unknown.

The proposed fixed-time algorithm can effectively solve the issues of finite-time control algorithms. In [26], a fixed-time control method was first presented to ensure that its convergence time was independent of the initial conditions of the system. In [27], a new fixed-time controller was presented to address the power system control issue, but the effect of disturbances on the system was not considered. In [28], a neural network-based fixed-time controller was raised to address the spacecraft attitude tracking issue. In [29], for spacecraft systems with disturbances and inertial uncertainties, a nonsingular fixed-time SM surface is designed, while an exponential function is introduced for the reaching law to improve it, and the issue of the unknown upper bound of disturbances is solved by the adaptive law technique, and simulations demonstrate the superiority of its control scheme. In [30], a fixed-time control method based on fuzzy control is proposed for the control of quadrotor unmanned aerial vehicles in the presence of actuator saturation, and a new SM surface is constructed to handle the singularity issue.

Inspired by the above-mentioned literature and aiming at the robotic manipulator system with unknown external disturbances, a nonsingular fixed-time controller based on adaptive law is proposed in this work. The main contributions are concluded as follows:

- (1) A new fixed-time SM surface is proposed, and a reaching law based on the arctangent function is designed to shorten the convergence time of the system variables and improve the accuracy.
- (2) The upper bound of the unknown disturbance is effectively estimated by the adaptive technique, which compensates for the impact brought by the unknown disturbance to the system.
- (3) The fixed-time convergence of the states is analyzed by rigorous theoretical proof.

This paper is organized as follows: “[Problem description and a priori knowledge](#)” gives the control object model and some basic lemmas; “[Adaptive fixed-time SM controller design](#)” analyzes the various components of the controller. “[Control system stability analysis](#)” demonstrates the stability of the adaptive fixed-time controller. “[Simulation case analysis](#)” gives a comparative analysis of the controllers proposed in this work. “[Conclusion](#)” provides the conclusion of this work.

## Problem description and a priori knowledge

### Prior knowledge

**Lemma 1** ([31]). *For any positive real numbers  $x_i, i = 1, 2, \dots, n$ , the following inequality holds:*

$$\sum_{i=1}^n x_i^{l_1} \geq \left( \sum_{i=1}^n x_i \right)^{l_1}, \quad (1)$$

$$\sum_{i=1}^n x_i^{l_2} \geq n^{1-l_2} \left( \sum_{i=1}^n x_i \right)^{l_2}, \quad (2)$$

where  $0 < l_1 \leq 1$  and  $l_2 > 1$ .

### Problem description

The robotic manipulator system model is represented as

$$\mathbf{M}(\mathbf{q})\ddot{\mathbf{q}} + \mathbf{C}(\mathbf{q}, \dot{\mathbf{q}})\dot{\mathbf{q}} + \mathbf{G}(\mathbf{q}) = \boldsymbol{\tau} + \boldsymbol{\tau}_d, \quad (3)$$

where  $\mathbf{q}$  and  $\dot{\mathbf{q}}$  are the joint position and velocity vectors, respectively, and  $\ddot{\mathbf{q}}$  represents the acceleration vector.  $\mathbf{M}(\mathbf{q})$  is the inertia matrix.  $\mathbf{C}(\mathbf{q}, \dot{\mathbf{q}})$  and  $\mathbf{G}(\mathbf{q})$  are the centrifugal Coriolis matrix and gravity vector, respectively.  $\boldsymbol{\tau}_d$  represents external disturbance.  $\boldsymbol{\tau}$  stands for control input torque.

The main objective of this research paper is to design a fixed-time robust controller to achieve fast convergence of the system state and improve its accuracy. Each part of the design of this paper is analyzed in detail below.

### Adaptive fixed-time SM controller design

In this section, the performance of the sliding and reaching phases is enhanced by designing a novel fixed-time SM surface and an enhanced reaching law, respectively. Then, the adaptive law is raised to handle the problem that the upper bound of the disturbance is unknown.

### Nonsingular fixed-time SM surface design

First, the tracking error is defined as  $\mathbf{e} = \mathbf{q} - \mathbf{q}_d$ , and  $\mathbf{q}_d$  is the desired trajectory. In response to the singularity issue of the traditional fixed-time SM surface [32], this paper designs a new type of SM surface that not only avoids the singularity issue but also enhances the error convergence accuracy and rate, which can be written as

$$\mathbf{s} = \dot{\mathbf{e}} + \alpha(\mathbf{e}) + \mathbf{c}_3\boldsymbol{\varphi}(\mathbf{e}), \quad (4)$$

where the  $i$ th term of  $\alpha(\mathbf{e})$  is  $\alpha(e_i)_i = c_{1i}e_i + c_{2i}|e_i|^{a_{1i}}\text{sign}(e_i)$ . The parameters  $c_{1i}$ ,  $c_{2i}$ ,  $c_{3i}$ , and  $a_{1i}$  fulfill

$c_{1i} > 0, c_{2i} > 0, c_{3i} > 0$ , and  $a_{1i} > 1$ . The singularity issue is handled by employing a piecewise function, and the  $i$ th term of  $\varphi(\mathbf{e})$  is expressed as

$$\varphi(e_i)_i = \begin{cases} |e_i|^{a_{2i}} \text{sign}(e_i), & \bar{s}_i = 0 \vee (\bar{s}_i \neq 0, |e_i| \geq \mu_i), \\ n_{1i}e_i + n_{2i}f(e_i)|e_i|^{a_{3i}} \text{sign}(e_i), & \bar{s}_i \neq 0, |e_i| < \mu_i, \end{cases} \tag{5}$$

where  $0.5 < a_{2i} < 1, 1 < a_{3i} < 2, f(e_i) = 1 + w_{1i} \cos\left(\frac{\pi e_i}{2\mu_i}\right), 0 \leq w_{1i} < \frac{2(a_{3i}-1)}{\pi}$ , and  $\mu_i > 0$ .  $\bar{s}_i$  is represented as

$$\bar{s}_i = \dot{e}_i + \alpha(e_i)_i + c_{3i}|e_i|^{a_{2i}} \text{sign}(e_i). \tag{6}$$

Since the function  $\varphi(\mathbf{e})$  is a piecewise function, to ensure the continuity of  $\varphi(\mathbf{e})$  and  $\dot{\varphi}(\mathbf{e})$ , the parameters  $n_{1i}$  and  $n_{2i}$  are designed as

$$n_{1i} = \frac{a_{3i} - \frac{\pi w_{1i}}{2} - a_{2i}}{a_{3i} - \frac{\pi w_{1i}}{2} - 1} \mu_i^{a_{2i}-1}, \tag{7}$$

$$n_{2i} = \frac{a_{2i} - 1}{a_{3i} - \frac{\pi w_{1i}}{2} - 1} \mu_i^{a_{2i}-a_{3i}}. \tag{8}$$

The function  $\dot{\varphi}(\mathbf{e})$  can be expressed as

$$\dot{\varphi}(e_i)_i = \begin{cases} a_{2i}\dot{e}_i |e_i|^{a_{2i}-1}, & \bar{s}_i = 0 \vee (\bar{s}_i \neq 0, |e_i| \geq \mu_i) \\ n_{1i}\dot{e}_i + f_a(e_i), & \bar{s}_i \neq 0, |e_i| < \mu_i \end{cases}$$

$$f_a(e_i) = n_{2i}a_{3i} \left(1 + w_{1i} \cos\left(\frac{\pi e_i}{2\mu_i}\right)\right) |e_i|^{a_{3i}-1} \dot{e}_i - n_{2i}w_{1i} \sin\left(\frac{\pi e_i}{2\mu_i}\right) |e_i|^{a_{3i}} \text{sign}(e_i) \frac{\pi \dot{e}_i}{2\mu_i}. \tag{9}$$

According to the range of values of  $a_{3i}$ , it is known that there exists  $a_{3i} - 1 > 0$ , and the SM surface raised in this paper does not undergo singularity. Bringing Eqs. (7) and (8) into Eqs. (9) and (5) shows that the function  $\varphi(\mathbf{e})$  and its first-order derivatives  $\dot{\varphi}(\mathbf{e})$  are continuous, which can effectively enhance the controller performance. The SM surface proposed in this work has a fast time convergence property in the whole phase. When  $\bar{s}_i = 0 \vee (\bar{s}_i \neq 0, |e_i| \geq \mu_i)$  is held, it is known that the SM surface is represented as

$$s_i = \dot{e}_i + c_{1i}e_i + c_{2i}|e_i|^{a_{1i}} \text{sign}(e_i) + c_{3i}|e_i|^{a_{2i}} \text{sign}(e_i). \tag{10}$$

When the system state satisfies  $s_i = \bar{s}_i = 0$ , Eq. (10) is expressed as

$$\dot{e}_i = -c_{1i}e_i - c_{2i}|e_i|^{a_{1i}} \text{sign}(e_i) - c_{3i}|e_i|^{a_{2i}} \text{sign}(e_i). \tag{11}$$

The parameters satisfy  $a_{1i} > 1$  and  $0.5 < a_{2i} < 1$ , and the system state has a better convergence rate both near and far from the zero point. To certify the simplicity of the paper, the

$i$ th DOF is used to verify its fixed convergence time property, and the design function is

$$V_{1i} = \frac{1}{2}e_i^2. \tag{12}$$

Taking first-order differentiation of Eq. (12) and bringing Eq. (11) into Eq. (12), we can get

$$\begin{aligned} \dot{V}_{1i} &= e_i \dot{e}_i \\ &= e_i(-c_{1i}e_i - c_{2i}|e_i|^{a_{1i}} \text{sign}(e_i) - c_{3i}|e_i|^{a_{2i}} \text{sign}(e_i)) \\ &= -c_{1i}e_i^2 - c_{2i}|e_i|^{a_{1i}+1} - c_{3i}|e_i|^{a_{2i}+1} \\ &= -2c_{1i}V_{1i} - c_{2i}2^{\frac{a_{1i}+1}{2}} V_{1i}^{\frac{a_{1i}+1}{2}} - 2^{\frac{a_{2i}+1}{2}} c_{3i} V_{1i}^{\frac{a_{2i}+1}{2}} \\ &= -\omega_1 V_{1i} - \omega_2 V_{1i}^{\frac{a_{1i}+1}{2}} - \omega_3 V_{1i}^{\frac{a_{2i}+1}{2}}, \end{aligned} \tag{13}$$

where  $\omega_1=2c_{1i}, \omega_2=c_{2i}2^{\frac{a_{1i}+1}{2}}$ , and  $\omega_3=2^{\frac{a_{2i}+1}{2}} c_{3i}$ . In the following, we will solve the differential Eq. (13), proving that  $V_{1i}(e_i) = 0$  can be reached at a fixed time. We can get

$$\begin{aligned} T_1 &\leq \lim_{V_{1i}(e_0) \rightarrow \infty} \int_0^{V_{1i}(e_0)} \frac{dV_{1i}}{\omega_1 V_{1i} + \omega_2 V_{1i}^{\frac{a_{1i}+1}{2}} + \omega_3 V_{1i}^{\frac{a_{2i}+1}{2}}} \\ &\leq \int_0^1 \frac{dV_{1i}}{\omega_1 V_{1i} + \omega_3 V_{1i}^{\frac{a_{2i}+1}{2}}} \\ &\quad + \lim_{V_{1i}(e_0) \rightarrow \infty} \int_1^{V_{1i}(e_0)} \frac{dV_{1i}}{\omega_1 V_{1i} + \omega_2 V_{1i}^{\frac{a_{1i}+1}{2}}} \\ &\leq \int_0^1 \frac{dV_{1i}}{\omega_1 V_{1i} + \omega_3 V_{1i}^{\frac{a_{2i}+1}{2}}} + \lim_{V_{1i}(e_0) \rightarrow \infty} \int_1^{V_{1i}(e_0)} \frac{dV_{1i}}{\omega_2 V_{1i}^{\frac{a_{1i}+1}{2}}} \\ &= \frac{2}{\omega_1(1 - a_{2i})} \ln\left(1 + \frac{\omega_1}{\omega_3}\right) + \frac{2}{\omega_2(a_{1i} - 1)}. \end{aligned} \tag{14}$$

Based on the above analysis, it is demonstrated that the error state will reach the balance point at a fixed time  $T_1$ .

**Remark 1.** Compared with the SM surface designed in [19, 23, 29, 30], which requires changes to the reaching law to eliminate the singularity, the SM surface presented in this work does not require adjustments to the reaching law, which can effectively accelerate the error convergence.

**Remark 2.** The SM surface Eq. (4) is inspired by [25]. Compared with [25], the SM surface Eq. (4) has a fixed-time convergence property, which does not rely on the size of the initial conditions of the system. The upper bound of the convergence time can be calculated according to the parameter gain. Also, the new error convergence term  $c_{2i}|e_i|^{a_{1i}} \text{sign}(e_i)$  added in Eq. (4) can further accelerate the error convergence.

### Design of reaching law

The fixed-time SM surface designed in the previous section is mainly for the sliding phase. To boost the performance of the reaching phase, a new reaching law is designed in this paper, which is defined as

$$\dot{s}_i = \frac{1}{\mathbf{N}(s_i)_i} \left[ -k_{1i} |s_i|^{b_{1i}} \text{sign}(s_i) - k_{2i} |s_i|^{b_{2i}} \text{sign}(s_i) \right] - k_{3i} s_i, \tag{15}$$

where  $\dot{s}_i$  is the  $i$ th term of  $\dot{\mathbf{s}}$ . The parameters  $b_{1i}$ ,  $b_{2i}$ ,  $k_{1i}$ ,  $k_{2i}$ , and  $k_{3i}$  satisfy  $b_{1i} > 1$ ,  $0 < b_{2i} < 1$ ,  $k_{1i} > 0$ ,  $k_{2i} > 0$ , and  $k_{3i} > 0$ . The  $\mathbf{N}(s_i)_i$  is expressed as

$$\mathbf{N}(s_i)_i = \left( h_{1i} - \arctan h_{2i} |s_i|^{h_{3i}} \right) h_{4i}, \tag{16}$$

where  $h_{1i} = \frac{\pi}{2}$ ,  $h_{2i} > 0$ ,  $0 < h_{3i} \leq 1$ , and  $h_{4i} > \frac{2}{\pi}$ . From Eq. (16), it can be seen that the function  $\mathbf{N}(s_i)_i$  is positive in any case and does not affect the control system stability. Further analysis shows that when the initial size of the SM variable is great, the parameter  $\arctan h_{2i} |s_i|^{h_{3i}}$  tends to  $\frac{\pi}{2}$ . At this time, it is made to satisfy  $0 < \mathbf{N}(s_i)_i < 1$  with a suitable choice of parameters. Then, the parameters  $\frac{k_{1i}}{\mathbf{N}(s_i)_i}$  and  $\frac{k_{2i}}{\mathbf{N}(s_i)_i}$  are larger than  $k_{1i}$  and  $k_{2i}$ , respectively, to speed up the convergence of the SM variables. When the initial size of the SM variable is small, the parameter  $\arctan h_{2i} |s_i|^{h_{3i}}$  is close to 0. At this time,  $\mathbf{N}(s_i)_i = \frac{\pi}{2} h_{4i}$  is greater than 1, which reduces the value of the parameters  $k_{1i}$  and  $k_{2i}$ . As a result, the convergence speed of the SM variable becomes slower, and the chattering phenomenon is reduced. According to the above analysis, it is easy to know that the value range of the arctangent function is between 0 and  $\frac{\pi}{2}$ . The size of the arctangent function can follow the size of the SM variable to make corresponding changes, thus changing the magnitude of the parameter  $\mathbf{N}(s_i)_i$ , which can effectively adjust the speed of convergence of the SM variable and balance the relationship between the speed of convergence and the size of the control input.

**Remark 3.** Increasing the amplitude of parameter  $h_{2i}$  or decreasing the amplitude of parameter  $h_{4i}$  can further lead to faster convergence, but will result in more chattering. Therefore, it is necessary to balance the relationship between the point convergence speed and the chattering magnitude and choose a more reasonable value.

### Design of the controller

Combining the SM surface Eq. (4) and the reaching law Eq. (15), the controller is

$$\tau = \mathbf{M}(\mathbf{q})\ddot{\mathbf{q}}_d + \mathbf{M}(\mathbf{q})(-\dot{\alpha}(\mathbf{e}) - c_3\dot{\phi}(\mathbf{e})) + \mathbf{C}(\mathbf{q}, \dot{\mathbf{q}})\dot{\mathbf{q}} + \mathbf{G}(\mathbf{q})$$

$$+ \mathbf{M}(\mathbf{q}) \left( -\frac{\mathbf{k}_1}{\mathbf{N}(\mathbf{s})} |\mathbf{s}|^{b_1} \text{sign}(\mathbf{s}) - \frac{\mathbf{k}_2}{\mathbf{N}(\mathbf{s})} |\mathbf{s}|^{b_2} \text{sign}(\mathbf{s}) - \mathbf{k}_3 \mathbf{s} - \mathbf{D} \right), \tag{17}$$

where  $\dot{\alpha}(\mathbf{e}) = \mathbf{c}_1 \dot{\mathbf{e}} + \mathbf{a}_1 \mathbf{c}_2 |\mathbf{e}|^{a_1-1} \dot{\mathbf{e}}$  and  $\mathbf{D} = \mathbf{M}(\mathbf{q})^{-1} \boldsymbol{\tau}_d$ . From [33], it is known that the disturbance  $\mathbf{D}$  satisfies the following inequality:

$$|D_i| \leq v_{1i} + v_{2i} |q_i| + v_{3i} |\dot{q}_i|^2, \tag{18}$$

where  $v_{1i}$ ,  $v_{2i}$ , and  $v_{3i}$  are all positive constants. In the actual situation,  $v_{1i}$ ,  $v_{2i}$ , and  $v_{3i}$  are unknown. The adaptive law is designed in this paper to estimate them, and the corresponding adaptive law is expressed as

$$\begin{aligned} \hat{v}_{1i} &= p_{1i} (|s_i| - m_{1i} \hat{v}_{1i}), \\ \hat{v}_{2i} &= p_{2i} (|s_i| |q_i| - m_{2i} \hat{v}_{2i}), \\ \hat{v}_{3i} &= p_{3i} (|s_i| |\dot{q}_i|^2 - m_{3i} \hat{v}_{3i}), \end{aligned} \tag{19}$$

where  $p_{1i} > 0$ ,  $p_{2i} > 0$ ,  $p_{3i} > 0$ ,  $m_{1i} > 0$ ,  $m_{2i} > 0$ , and  $m_{3i} > 0$ .  $\hat{v}_{1i}$ ,  $\hat{v}_{2i}$ , and  $\hat{v}_{3i}$  represent the estimated values of  $v_{1i}$ ,  $v_{2i}$ , and  $v_{3i}$ , respectively.

Combining Eq. (19) and controller (17), we get

$$\begin{aligned} \tau &= \mathbf{M}(\mathbf{q})\ddot{\mathbf{q}}_d + \mathbf{M}(\mathbf{q})(-\dot{\alpha}(\mathbf{e}) - c_3\dot{\phi}(\mathbf{e})) + \mathbf{C}(\mathbf{q}, \dot{\mathbf{q}})\dot{\mathbf{q}} + \mathbf{G}(\mathbf{q}) \\ &+ \mathbf{M}(\mathbf{q}) \left( -\frac{\mathbf{k}_1}{\mathbf{N}(\mathbf{s})} |\mathbf{s}|^{b_1} \text{sign}(\mathbf{s}) - \frac{\mathbf{k}_2}{\mathbf{N}(\mathbf{s})} |\mathbf{s}|^{b_2} \text{sign}(\mathbf{s}) - \mathbf{k}_3 \mathbf{s} \right. \\ &\quad \left. - (\hat{v}_1 + \hat{v}_2 |\mathbf{q}| + \hat{v}_3 |\dot{\mathbf{q}}|^2) \text{sign}(\mathbf{s}) \right). \end{aligned} \tag{20}$$

**Remark 4.** For the adaptive law Eq. (19), when increasing its coefficients  $p_{1i}$ ,  $p_{2i}$ , and  $p_{3i}$ , it will speed up its parameter estimation and approach the upper bound of the disturbance more quickly, but too high an estimation speed may have adverse effects. Smaller parameters  $m_{1i}$ ,  $m_{2i}$ , and  $m_{3i}$  can maintain a faster upper bound estimation rate for disturbances, but introduce an increase in the control input amplitude. According to the above analysis, the influence of different factors needs to be taken into account when adjusting the parameters.

### Control system stability analysis

In this section, the fixed-time stability of the sliding phase and the reaching phase is analyzed separately. For the sake of simplicity in the proof, we will choose the  $i$ th DOF for the proof, and the Lyapunov function is selected as

$$V_{2i} = \frac{1}{2} s_i^2 + \frac{1}{2p_{1i}} \tilde{v}_{1i}^2 + \frac{1}{2p_{2i}} \tilde{v}_{2i}^2 + \frac{1}{2p_{3i}} \tilde{v}_{3i}^2, \tag{21}$$

where  $\tilde{v}_{1i} = v_{1i} - \hat{v}_{1i}$ ,  $\tilde{v}_{2i} = v_{2i} - \hat{v}_{2i}$ , and  $\tilde{v}_{3i} = v_{3i} - \hat{v}_{3i}$ . The derivation of Eq. (21) yields

$$\dot{V}_{2i} = s_i \dot{s}_i + \frac{1}{p_{1i}} \tilde{v}_{1i} \dot{\tilde{v}}_{1i} + \frac{1}{p_{2i}} \tilde{v}_{2i} \dot{\tilde{v}}_{2i} + \frac{1}{p_{3i}} \tilde{v}_{3i} \dot{\tilde{v}}_{3i}. \tag{22}$$

A first-order derivative of the SM surface Eq. (4) yields

$$\begin{aligned} \dot{s} &= \ddot{e} + \dot{\alpha}(e) + c_3 \dot{\phi}(e) \\ &= \ddot{q} - \ddot{q}_d + \dot{\alpha}(e) + c_3 \dot{\phi}(e) \\ &= \mathbf{M}(\mathbf{q})^{-1} (\boldsymbol{\tau} + \boldsymbol{\tau}_d - \mathbf{C}(\mathbf{q}, \dot{\mathbf{q}})\dot{\mathbf{q}} - \mathbf{G}(\mathbf{q})) - \ddot{q}_d + \dot{\alpha}(e) + c_3 \dot{\phi}(e). \end{aligned} \tag{23}$$

Bringing the control input Eq. (20) into Eq. (23) for simplification, and combining it with Eq. (22), we get

$$\begin{aligned} \dot{V}_{2i} &= s_i \dot{s}_i + \frac{1}{p_{1i}} \tilde{v}_{1i} \dot{\tilde{v}}_{1i} + \frac{1}{p_{2i}} \tilde{v}_{2i} \dot{\tilde{v}}_{2i} + \frac{1}{p_{3i}} \tilde{v}_{3i} \dot{\tilde{v}}_{3i} \\ &= s_i \left( -\frac{k_{1i}}{\mathbf{N}(s_i)_i} |s_i|^{b_{1i}} \text{sign}(s_i) - \frac{k_{2i}}{\mathbf{N}(s_i)_i} |s_i|^{b_{2i}} \text{sign}(s_i) \right. \\ &\quad \left. - k_{3i} s_i - (\hat{v}_{1i} + \hat{v}_{2i} |q_i| + \hat{v}_{3i} |\dot{q}_i|^2) \text{sign}(s_i) + D_i \right) \\ &\quad + \frac{1}{p_{1i}} \tilde{v}_{1i} \dot{\tilde{v}}_{1i} + \frac{1}{p_{2i}} \tilde{v}_{2i} \dot{\tilde{v}}_{2i} + \frac{1}{p_{3i}} \tilde{v}_{3i} \dot{\tilde{v}}_{3i}. \end{aligned} \tag{24}$$

Bringing the adaptive law Eq. (19) into Eq. (24) yields

$$\begin{aligned} \dot{V}_{2i} &= s_i \dot{s}_i + \frac{1}{p_{1i}} \tilde{v}_{1i} \dot{\tilde{v}}_{1i} + \frac{1}{p_{2i}} \tilde{v}_{2i} \dot{\tilde{v}}_{2i} + \frac{1}{p_{3i}} \tilde{v}_{3i} \dot{\tilde{v}}_{3i} \\ &= s_i \left( -\frac{k_{1i}}{\mathbf{N}(s_i)_i} |s_i|^{b_{1i}} \text{sign}(s_i) - \frac{k_{2i}}{\mathbf{N}(s_i)_i} |s_i|^{b_{2i}} \text{sign}(s_i) - k_{3i} s_i - (\hat{v}_{1i} + \hat{v}_{2i} |q_i| + \hat{v}_{3i} |\dot{q}_i|^2) \text{sign}(s_i) + D_i \right) \\ &\quad - \frac{1}{p_{1i}} \tilde{v}_{1i} (p_{1i} (|s_i| - m_{1i} \hat{v}_{1i})) - \frac{1}{p_{2i}} \tilde{v}_{2i} (p_{2i} (|s_i| |q_i| - m_{2i} \hat{v}_{2i})) - \frac{1}{p_{3i}} \tilde{v}_{3i} (p_{3i} (|s_i| |\dot{q}_i|^2 - m_{3i} \hat{v}_{3i})) \\ &= s_i \left( -\frac{k_{1i}}{\mathbf{N}(s_i)_i} |s_i|^{b_{1i}} \text{sign}(s_i) - \frac{k_{2i}}{\mathbf{N}(s_i)_i} |s_i|^{b_{2i}} \text{sign}(s_i) - k_{3i} s_i - (\hat{v}_{1i} + \hat{v}_{2i} |q_i| + \hat{v}_{3i} |\dot{q}_i|^2) \text{sign}(s_i) + D_i \right) - \tilde{v}_{1i} |s_i| \\ &\quad + m_{1i} \hat{v}_{1i} \tilde{v}_{1i} - \tilde{v}_{2i} |s_i| |q_i| + m_{2i} \hat{v}_{2i} \tilde{v}_{2i} - \tilde{v}_{3i} |s_i| |\dot{q}_i|^2 + m_{3i} \hat{v}_{3i} \tilde{v}_{3i} \\ &= s_i \left( -\frac{k_{1i}}{\mathbf{N}(s_i)_i} |s_i|^{b_{1i}} \text{sign}(s_i) - \frac{k_{2i}}{\mathbf{N}(s_i)_i} |s_i|^{b_{2i}} \text{sign}(s_i) - k_{3i} s_i + D_i \right) + m_{1i} \hat{v}_{1i} \tilde{v}_{1i} + m_{2i} \hat{v}_{2i} \tilde{v}_{2i} + m_{3i} \hat{v}_{3i} \tilde{v}_{3i} - v_{1i} |s_i| \\ &\quad - v_{2i} |s_i| |q_i| - v_{3i} |s_i| |\dot{q}_i|^2 \\ &\leq s_i \left( -\frac{k_{1i}}{\mathbf{N}(s_i)_i} |s_i|^{b_{1i}} \text{sign}(s_i) - \frac{k_{2i}}{\mathbf{N}(s_i)_i} |s_i|^{b_{2i}} \text{sign}(s_i) - k_{3i} s_i \right) + |s_i| |D_i| - v_{1i} |s_i| - v_{2i} |s_i| |q_i| - v_{3i} |s_i| |\dot{q}_i|^2 \\ &\quad + m_{1i} \hat{v}_{1i} \tilde{v}_{1i} + m_{2i} \hat{v}_{2i} \tilde{v}_{2i} + m_{3i} \hat{v}_{3i} \tilde{v}_{3i} \\ &\leq s_i \left( -\frac{k_{1i}}{\mathbf{N}(s_i)_i} |s_i|^{b_{1i}} \text{sign}(s_i) - \frac{k_{2i}}{\mathbf{N}(s_i)_i} |s_i|^{b_{2i}} \text{sign}(s_i) - k_{3i} s_i \right) + m_{1i} \hat{v}_{1i} \tilde{v}_{1i} + m_{2i} \hat{v}_{2i} \tilde{v}_{2i} + m_{3i} \hat{v}_{3i} \tilde{v}_{3i}. \end{aligned} \tag{25}$$

Equation (25) can be further simplified as

$$\begin{aligned} \dot{V}_{2i} &\leq s_i \left( -\frac{k_{1i}}{\mathbf{N}(s_i)_i} |s_i|^{b_{1i}} \text{sign}(s_i) - \frac{k_{2i}}{\mathbf{N}(s_i)_i} |s_i|^{b_{2i}} \text{sign}(s_i) - k_{3i} s_i \right) \\ &\quad + m_{1i} \hat{v}_{1i} \tilde{v}_{1i} + m_{2i} \hat{v}_{2i} \tilde{v}_{2i} + m_{3i} \hat{v}_{3i} \tilde{v}_{3i} \\ &= -k_{4i} |s_i|^{b_{1i}+1} - k_{5i} |s_i|^{b_{2i}+1} - k_{3i} s_i^2 \\ &\quad + m_{1i} \hat{v}_{1i} \tilde{v}_{1i} + m_{2i} \hat{v}_{2i} \tilde{v}_{2i} + m_{3i} \hat{v}_{3i} \tilde{v}_{3i}, \end{aligned} \tag{26}$$

where  $k_{4i} = \frac{k_{1i}}{\mathbf{N}(s_i)_i}$  and  $k_{5i} = \frac{k_{2i}}{\mathbf{N}(s_i)_i}$ . The following relationships exist:

$$\begin{aligned} m_{1i} \hat{v}_{1i} \tilde{v}_{1i} &= m_{1i} \tilde{v}_{1i} (-\tilde{v}_{1i} + v_{1i}) \\ &\leq -\frac{m_{1i}(2\delta_1 - 1)}{2\delta_1} \tilde{v}_{1i}^2 + \frac{m_{1i}\delta_1}{2} v_{1i}^2, \end{aligned} \tag{27}$$

$$\begin{aligned} m_{2i} \hat{v}_{2i} \tilde{v}_{2i} &= m_{2i} \tilde{v}_{2i} (-\tilde{v}_{2i} + v_{2i}) \\ &\leq -\frac{m_{2i}(2\delta_2 - 1)}{2\delta_2} \tilde{v}_{2i}^2 + \frac{m_{2i}\delta_2}{2} v_{2i}^2, \end{aligned} \tag{28}$$

$$\begin{aligned} m_{3i} \hat{v}_{3i} \tilde{v}_{3i} &= m_{3i} \tilde{v}_{3i} (-\tilde{v}_{3i} + v_{3i}) \\ &\leq -\frac{m_{3i}(2\delta_3 - 1)}{2\delta_3} \tilde{v}_{3i}^2 + \frac{m_{3i}\delta_3}{2} v_{3i}^2, \end{aligned} \tag{29}$$

where  $\delta_1 > \frac{1}{2}$ ,  $\delta_2 > \frac{1}{2}$ , and  $\delta_3 > \frac{1}{2}$ . Bringing Eqs. (27)–(29) into Eq. (26), we get

$$\begin{aligned} \dot{V}_{2i} &\leq -k_{4i} |s_i|^{b_{1i}+1} - k_{5i} |s_i|^{b_{2i}+1} - k_{3i} s_i^2 \\ &\quad + m_{1i} \hat{v}_{1i} \tilde{v}_{1i} + m_{2i} \hat{v}_{2i} \tilde{v}_{2i} + m_{3i} \hat{v}_{3i} \tilde{v}_{3i} \\ &\leq -k_{4i} |s_i|^{b_{1i}+1} - k_{5i} |s_i|^{b_{2i}+1} - k_{3i} s_i^2 \\ &\quad - \frac{m_{1i}(2\delta_1 - 1)}{2\delta_1} \tilde{v}_{1i}^2 + \frac{m_{1i}\delta_1}{2} v_{1i}^2 - \frac{m_{2i}(2\delta_2 - 1)}{2\delta_2} \tilde{v}_{2i}^2 \\ &\quad + \frac{m_{2i}\delta_2}{2} v_{2i}^2 - \frac{m_{3i}(2\delta_3 - 1)}{2\delta_3} \tilde{v}_{3i}^2 + \frac{m_{3i}\delta_3}{2} v_{3i}^2 \end{aligned}$$

$$\begin{aligned}
 &\leq -k_{3i}s_i^2 - \frac{m_{1i}(2\delta_1 - 1)}{2\delta_1 p_{1i}} p_{1i} \tilde{v}_{1i}^2 + \frac{m_{1i}\delta_1}{2} v_{1i}^2 \\
 &\quad - \frac{m_{2i}(2\delta_2 - 1)}{2\delta_2 p_{2i}} p_{2i} \tilde{v}_{2i}^2 + \frac{m_{2i}\delta_2}{2} v_{2i}^2 \\
 &\quad - \frac{m_{3i}(2\delta_3 - 1)}{2\delta_3 p_{3i}} p_{3i} \tilde{v}_{3i}^2 + \frac{m_{3i}\delta_3}{2} v_{3i}^2 \\
 &\leq -k_{6i} \left( \frac{1}{2} s_i^2 + \frac{1}{2p_{1i}} \tilde{v}_{1i}^2 + \frac{1}{2p_{2i}} \tilde{v}_{2i}^2 + \frac{1}{2p_{3i}} \tilde{v}_{3i}^2 \right) \\
 &\quad + \frac{m_{1i}\delta_1}{2} v_{1i}^2 + \frac{m_{2i}\delta_2}{2} v_{2i}^2 + \frac{m_{3i}\delta_3}{2} v_{3i}^2 \\
 &\leq -k_{6i} V_{2i} + \varpi_{1i}, \tag{30}
 \end{aligned}$$

where  $k_{6i} = \min(2k_{3i}, \frac{m_{1i}(2\delta_1-1)}{\delta_1} p_{1i}, \frac{m_{2i}(2\delta_2-1)}{\delta_2} p_{2i}, \frac{m_{3i}(2\delta_3-1)}{\delta_3} p_{3i})$  and  $\varpi_{1i} = \frac{m_{1i}\delta_1}{2} v_{1i}^2 + \frac{m_{2i}\delta_2}{2} v_{2i}^2 + \frac{m_{3i}\delta_3}{2} v_{3i}^2$ . According to the previous analysis, it is known that the parameters  $s_i, \tilde{v}_{1i}, \tilde{v}_{2i}$ , and  $\tilde{v}_{3i}$  are bounded. The parameters  $\hat{v}_{1i}, \hat{v}_{2i}$ , and  $\hat{v}_{3i}$  are bounded. From Eq. (30), we can get

$$\begin{aligned}
 \dot{V}_{2i} &\leq -k_{4i} |s_i|^{b_{1i}+1} - k_{5i} |s_i|^{b_{2i}+1} - k_{3i} s_i^2 \\
 &\quad + m_{1i} \hat{v}_{1i} \tilde{v}_{1i} + m_{2i} \hat{v}_{2i} \tilde{v}_{2i} + m_{3i} \hat{v}_{3i} \tilde{v}_{3i} \\
 &= -k_{4i} 2^{\frac{b_{1i}+1}{2}} \left( \frac{1}{2} s_i^2 \right)^{\frac{b_{1i}+1}{2}} - k_{5i} 2^{\frac{b_{2i}+1}{2}} \left( \frac{1}{2} s_i^2 \right)^{\frac{b_{2i}+1}{2}} \\
 &\quad - 2k_{3i} \left( \frac{1}{2} s_i^2 \right) + \left( \frac{1}{2p_{1i}} \tilde{v}_{1i}^2 \right)^{\frac{b_{1i}+1}{2}} \\
 &\quad + \left( \frac{1}{2p_{2i}} \tilde{v}_{2i}^2 \right)^{\frac{b_{1i}+1}{2}} + \left( \frac{1}{2p_{3i}} \tilde{v}_{3i}^2 \right)^{\frac{b_{1i}+1}{2}} \\
 &\quad + \left( \frac{1}{2p_{1i}} \tilde{v}_{1i}^2 \right)^{\frac{b_{2i}+1}{2}} + \left( \frac{1}{2p_{2i}} \tilde{v}_{2i}^2 \right)^{\frac{b_{2i}+1}{2}} \\
 &\quad + \left( \frac{1}{2p_{3i}} \tilde{v}_{3i}^2 \right)^{\frac{b_{2i}+1}{2}} + \left( \frac{1}{2p_{1i}} \tilde{v}_{1i}^2 \right) + \left( \frac{1}{2p_{2i}} \tilde{v}_{2i}^2 \right) \\
 &\quad + \left( \frac{1}{2p_{3i}} \tilde{v}_{3i}^2 \right) - \left( \frac{1}{2p_{1i}} \tilde{v}_{1i}^2 \right)^{\frac{b_{1i}+1}{2}} \\
 &\quad - \left( \frac{1}{2p_{2i}} \tilde{v}_{2i}^2 \right)^{\frac{b_{1i}+1}{2}} - \left( \frac{1}{2p_{3i}} \tilde{v}_{3i}^2 \right)^{\frac{b_{1i}+1}{2}} \\
 &\quad - \left( \frac{1}{2p_{1i}} \tilde{v}_{1i}^2 \right)^{\frac{b_{2i}+1}{2}} - \left( \frac{1}{2p_{2i}} \tilde{v}_{2i}^2 \right)^{\frac{b_{2i}+1}{2}} \\
 &\quad - \left( \frac{1}{2p_{3i}} \tilde{v}_{3i}^2 \right)^{\frac{b_{2i}+1}{2}} - \left( \frac{1}{2p_{1i}} \tilde{v}_{1i}^2 \right) - \left( \frac{1}{2p_{2i}} \tilde{v}_{2i}^2 \right) \\
 &\quad - \left( \frac{1}{2p_{3i}} \tilde{v}_{3i}^2 \right) + m_{1i} \hat{v}_{1i} \tilde{v}_{1i} + m_{2i} \hat{v}_{2i} \tilde{v}_{2i} + m_{3i} \hat{v}_{3i} \tilde{v}_{3i} \\
 &\leq -k_{7i} \left( \left( \frac{1}{2} s_i^2 \right)^{\frac{b_{1i}+1}{2}} + \left( \frac{1}{2p_{1i}} \tilde{v}_{1i}^2 \right)^{\frac{b_{1i}+1}{2}} + \left( \frac{1}{2p_{2i}} \tilde{v}_{2i}^2 \right)^{\frac{b_{1i}+1}{2}} \right. \\
 &\quad \left. + \left( \frac{1}{2p_{3i}} \tilde{v}_{3i}^2 \right)^{\frac{b_{1i}+1}{2}} \right) - k_{8i} \left( \left( \frac{1}{2} s_i^2 \right)^{\frac{b_{2i}+1}{2}} \right.
 \end{aligned}$$

where  $k_{7i} = \min(k_{4i} 2^{\frac{b_{1i}+1}{2}}, 1)$ ,  $k_{8i} = \min(k_{5i} 2^{\frac{b_{2i}+1}{2}}, 1)$ , and  $k_{9i} = \min(2k_{3i}, 1)$ . According to the previous analysis, it is clear that  $\varpi_{2i}$  is bound as a whole.  $\varpi_{2i}$  can be expressed as

$$\begin{aligned}
 \varpi_{2i} &= |m_{1i} \hat{v}_{1i} \tilde{v}_{1i}| + |m_{2i} \hat{v}_{2i} \tilde{v}_{2i}| + |m_{3i} \hat{v}_{3i} \tilde{v}_{3i}| \\
 &\quad + \left( \frac{1}{2p_{1i}} \tilde{v}_{1i}^2 \right)^{\frac{b_{1i}+1}{2}} + \left( \frac{1}{2p_{2i}} \tilde{v}_{2i}^2 \right)^{\frac{b_{1i}+1}{2}} + \left( \frac{1}{2p_{3i}} \tilde{v}_{3i}^2 \right)^{\frac{b_{1i}+1}{2}} \\
 &\quad + \left( \frac{1}{2p_{1i}} \tilde{v}_{1i}^2 \right)^{\frac{b_{2i}+1}{2}} + \left( \frac{1}{2p_{2i}} \tilde{v}_{2i}^2 \right)^{\frac{b_{2i}+1}{2}} + \left( \frac{1}{2p_{3i}} \tilde{v}_{3i}^2 \right)^{\frac{b_{2i}+1}{2}} \\
 &\quad + \left( \frac{1}{2p_{1i}} \tilde{v}_{1i}^2 \right) + \left( \frac{1}{2p_{2i}} \tilde{v}_{2i}^2 \right) + \left( \frac{1}{2p_{3i}} \tilde{v}_{3i}^2 \right). \tag{32}
 \end{aligned}$$

Considering the parameters satisfy  $\frac{b_{1i}+1}{2} > 1$  and  $0 < \frac{b_{2i}+1}{2} < 1$ , and combined with Lemma 1, we have

$$\begin{aligned}
 \dot{V}_{2i} &\leq -k_{7i} 4^{\frac{1-b_{1i}}{2}} (V_{2i})^{\frac{b_{1i}+1}{2}} - k_{8i} (V_{2i})^{\frac{b_{2i}+1}{2}} - k_{9i} V_{2i} + \varpi_{2i} \\
 &= -k_{10i} (V_{2i})^{\frac{b_{1i}+1}{2}} - k_{8i} (V_{2i})^{\frac{b_{2i}+1}{2}} - k_{9i} V_{2i} + \varpi_{2i}, \tag{33}
 \end{aligned}$$

where  $k_{10i} = k_{7i} 4^{\frac{1-b_{1i}}{2}}$ . For inequality (33), it can be transformed into the following three forms:

$$\begin{aligned}
 \dot{V}_{2i} &\leq -(1 - \theta_0) k_{10i} (V_{2i})^{\frac{b_{1i}+1}{2}} - \theta_0 k_{10i} (V_{2i})^{\frac{b_{1i}+1}{2}} \\
 &\quad - k_{8i} (V_{2i})^{\frac{b_{2i}+1}{2}} - k_{9i} V_{2i} + \varpi_{2i}, \tag{34}
 \end{aligned}$$

$$\begin{aligned}
 \dot{V}_{2i} &\leq -k_{10i} (V_{2i})^{\frac{b_{1i}+1}{2}} - (1 - \theta_0) k_{8i} (V_{2i})^{\frac{b_{2i}+1}{2}} \\
 &\quad - \theta_0 k_{8i} (V_{2i})^{\frac{b_{2i}+1}{2}} - k_{9i} V_{2i} + \varpi_{2i}, \tag{35}
 \end{aligned}$$

$$\begin{aligned}
 \dot{V}_{2i} &\leq -k_{10i} (V_{2i})^{\frac{b_{1i}+1}{2}} - k_{8i} (V_{2i})^{\frac{b_{2i}+1}{2}} \\
 &\quad - (1 - \theta_0) k_{9i} (V_{2i}) - \theta_0 k_{9i} V_{2i} + \varpi_{2i}, \tag{36}
 \end{aligned}$$

where  $0 < \theta_0 < 1$ . For Eq. (34), when  $-(1 - \theta_0) k_{10i} (V_{2i})^{\frac{b_{1i}+1}{2}} + \varpi_{2i} \leq 0$  is satisfied, Eq. (34) becomes

$$\dot{V}_{2i} \leq -\theta_0 k_{10i} (V_{2i})^{\frac{b_{1i}+1}{2}} - k_{8i} (V_{2i})^{\frac{b_{2i}+1}{2}} - k_{9i} (V_{2i}). \quad (37)$$

According to the previous analysis, Eq. (37) has the same form as Eq. (13), and the system state  $s_i$  will converge to

$$\left\{ \lim_{t \rightarrow T_{2a}} |s_i| \leq \sqrt{2 \left( \frac{\varpi_{2i}}{k_{10i}(1-\theta_0)} \right)^{\frac{2}{b_{1i}+1}}} \right\}. \quad (38)$$

$T_{2a}$  can be expressed as

$$T_{2a} \leq \frac{2 \ln \left( 1 + \frac{k_{9i}}{k_{8i}} \right)}{k_{9i}(1-b_{2i})} + \frac{2}{k_{10i}\theta_0(b_{1i}-1)}. \quad (39)$$

Doing a similar analysis for Eqs. (35) and (36), the final SM variables will converge to the following region:

$$\Delta_1 = \left\{ \lim_{t \rightarrow T_2} s_i \mid |s_i| \leq \min \left\{ \sqrt{2 \left( \frac{\varpi_{2i}}{k_{10i}(1-\theta_0)} \right)^{\frac{2}{b_{1i}+1}}}, \sqrt{2 \left( \frac{\varpi_{2i}}{k_{8i}(1-\theta_0)} \right)^{\frac{2}{b_{2i}+1}}}, \sqrt{2 \left( \frac{\varpi_{2i}}{k_{9i}(1-\theta_0)} \right)} \right\} \right\}. \quad (40)$$

The fixed convergence upper bound time  $T_2$  is denoted as

$$T_2 \leq \max \left\{ \frac{2 \ln \left( 1 + \frac{k_{9i}}{\theta_0 k_{8i}} \right)}{k_{9i}(1-b_{2i})} + \frac{2}{k_{10i}(b_{1i}-1)}, \frac{2 \ln \left( 1 + \frac{k_{9i}}{k_{8i}} \right)}{k_{9i}(1-b_{2i})} + \frac{2}{\theta_0 k_{10i}(b_{1i}-1)}, \frac{2 \ln \left( 1 + \frac{\theta_0 k_{9i}}{k_{8i}} \right)}{\theta_0 k_{9i}(1-b_{2i})} + \frac{2}{k_{10i}(b_{1i}-1)} \right\}. \quad (41)$$

According to the above analysis, the SM variables will reach the region at a fixed time  $T_2$ . The above analysis is mainly for the reaching phase, and the following analysis will be performed for the sliding phase. When  $|s_i| \leq \Delta_1$  is satisfied, the discussion can be divided into three cases at this point. When  $\bar{s}_i = 0$  is satisfied, it is known from the previous analysis that the system state will converge to zero at a fixed time. When  $\bar{s}_i = 0 \vee (\bar{s}_i \neq 0, |e_i| \geq \mu_i)$  is satisfied, then the SM surface is written as

$$s_i = \dot{e}_i + c_{1i} e_i + c_{2i} |e_i|^{a_{1i}} \text{sign}(e_i) + c_{3i} |e_i|^{a_{2i}} \text{sign}(e_i). \quad (42)$$

Equation (42) can be written in a different form and can be transformed as

$$\dot{e}_i + \left( c_{1i} - \frac{s_i}{e_i} \right) e_i + c_{2i} |e_i|^{a_{1i}} \text{sign}(e_i) + c_{3i} |e_i|^{a_{2i}} \text{sign}(e_i) = 0, \quad (43)$$

$$\dot{e}_i + c_{1i} e_i + \left( c_{2i} - \frac{s}{|e_i|^{a_{1i}} \text{sign}(e_i)} \right) |e_i|^{a_{1i}} \text{sign}(e_i) + c_{3i} |e_i|^{a_{2i}} \text{sign}(e_i) = 0, \quad (44)$$

$$\dot{e}_i + c_{1i} e_i + c_{2i} |e_i|^{a_{1i}} \text{sign}(e_i) + \left( c_{3i} - \frac{s_i}{|e_i|^{a_{2i}} \text{sign}(e_i)} \right) |e_i|^{a_{2i}} \text{sign}(e_i) = 0. \quad (45)$$

According to Eq. (43), when satisfied with  $\left( c_{1i} - \frac{s_i}{e_i} \right) > 0$ , Eq. (43) has the same form as Eq. (11), and the system state can converge at a fixed time to

$$|e_i| \leq \frac{|s_i|}{c_{1i}} \leq \frac{\Delta_1}{c_{1i}}. \quad (46)$$

Performing the same analysis for Eqs. (44) and (45), the system variables will converge at a fixed time to

$$|e_i| \leq \left( \frac{|s_i|}{c_{2i}} \right)^{\frac{1}{a_{1i}}} \leq \left( \frac{\Delta_1}{c_{2i}} \right)^{\frac{1}{a_{1i}}}, \quad (47)$$

$$|e_i| \leq \left( \frac{|s_i|}{c_{3i}} \right)^{\frac{1}{a_{2i}}} \leq \left( \frac{\Delta_1}{c_{3i}} \right)^{\frac{1}{a_{2i}}}. \quad (48)$$

According to the above analysis, the variable  $e_i$  will converge at a fixed time  $T_1$  to

$$|e_i| \leq \Delta_{2i} = \min \left\{ \max \left\{ \left( \mu_i, \frac{\Delta_1}{c_{1i}} \right) \right\}, \left\{ \left( \mu_i, \left( \frac{\Delta_1}{c_{2i}} \right)^{\frac{1}{a_{1i}}} \right) \right\}, \left\{ \left( \mu_i, \left( \frac{\Delta_1}{c_{3i}} \right)^{\frac{1}{a_{2i}}} \right) \right\} \right\}. \quad (49)$$

When the system state satisfies  $\bar{s}_i \neq 0, |e_i| < \mu_i$ , the error variable is already included in Eq. (49) at this point. In summary, the controller raised in this work has fixed-time convergence characteristics.

**Remark 5.** Compared to [17, 20, 24], the controller proposed in this work has a fixed-time characteristic. According to Eqs. (14) and (41), it can be seen that the convergence upper

bound time depends on the coefficient size and does not rely on the initial conditions of the system, which can be applied to a broader range of nonlinear systems and has a certain superiority.

**Remark 6.** Considering that the controller Eq. (20) designed in this paper is discontinuous and the control law contains switching functions, this problem can be improved by the saturation function.

**Remark 7.** For the reaching stage, the analysis of convergence time Eq. (40) and range Eq. (41) shows that increasing the reaching law coefficients  $k_{1i}$ ,  $k_{2i}$ , and  $k_{3i}$  can enhance the convergence speed and accuracy of the SM variables, but at the same time, chattering phenomena, high control input amplitude, and overshoot phenomena will occur.

For the sliding stage, the analysis of the convergence time of the SM surface Eq. (14) and the control accuracy Eq. (49) show that when increasing the SM surface coefficients  $c_{1i}$ ,  $c_{2i}$ , and  $c_{3i}$ , the convergence speed and accuracy of the tracking error can be effectively raised, but at the same time, the control input size will also be increased. When decreasing the SM surface coefficients  $c_{1i}$ ,  $c_{2i}$ , and  $c_{3i}$ , it slows down the convergence speed and accuracy of the tracking error and decreases the control input size. When the initial error size is large, we can both relatively increase the size of  $a_{1i}$  and decrease the size of  $a_{2i}$  to accelerate the error convergence and improve the control performance. Considering that the parameter  $\mu_i$  has an important influence on the system accuracy, we can gradually decrease it from a larger value until the control accuracy decreases and select it as an appropriate value.

According to the above analysis, the parameter size plays an important role in control performance. This paper currently follows the above rules and then, through repeated experiments, finally selects a more reasonable value to obtain a better tracking performance. In the future, we will consider developing a parameter adjustment mechanism to resize the size of the control parameters to obtain a more concise adjustment method, which is one of the future research contents.

## Simulation case analysis

To prove the advantages of the controller developed in this paper, the control scheme presented in this paper is compared with controllers from different works of literature. The two-joint robotic manipulator is the control target, and the model parameters are referred to [34]. The control scheme developed in this work is used as controller 1, the scheme corresponding to [24] is used as controller 2, the controller corresponding to [35] is used as controller 3, and the controller corresponding to [36] is used as controller 4, which are analyzed separately below.

In controller 2, the SM surface and reaching law are expressed as

$$\mathbf{s} = \dot{\mathbf{e}} + \mathbf{c}_1 \mathbf{e} + \mathbf{c}_3 \boldsymbol{\varphi}(\mathbf{e}), \quad (50)$$

$$\boldsymbol{\varphi}(e_i)_i = \begin{cases} |e_i|^{a_{2i}} \text{sign}(e_i), & \bar{s}_i = 0 \vee (\bar{s}_i \neq 0, |e_i| \geq \mu_i), \\ r_{1i} e_i + r_{2i} |e_i|^{a_{3i}} \text{sign}(e_i), & \bar{s}_i \neq 0, |e_i| < \mu_i, \end{cases} \quad (51)$$

$$\dot{\mathbf{s}} = -\mathbf{k}_2 |\mathbf{s}|^{b_2} \text{sign}(\mathbf{s}) - \mathbf{k}_3 \mathbf{s}, \quad (52)$$

where  $\bar{s}_i = \dot{e}_i + c_{1i} e_i + c_{2i} |e_i|^{a_{2i}} \text{sign}(e_i)$ . Parameters  $r_{1i}$  and  $r_{2i}$  refer to the [24]. Combining with the adaptive law proposed in this paper, controller 2 is

$$\begin{aligned} \tau = & \mathbf{M}(\mathbf{q})\ddot{\mathbf{q}}_d + \mathbf{M}(\mathbf{q})(-\mathbf{c}_1 \dot{\mathbf{e}} - \mathbf{c}_3 \dot{\boldsymbol{\varphi}}(\mathbf{e})) + \mathbf{C}(\mathbf{q}, \dot{\mathbf{q}})\dot{\mathbf{q}} + \mathbf{G}(\mathbf{q}) \\ & + \mathbf{M}(\mathbf{q}) \left( -\mathbf{k}_2 |\mathbf{s}|^{b_2} \text{sign}(\mathbf{s}) - \mathbf{k}_3 \mathbf{s} - \left( \hat{\mathbf{v}}_1 + \hat{\mathbf{v}}_2 |\mathbf{q}| + \hat{\mathbf{v}}_3 |\dot{\mathbf{q}}|^2 \right) \text{sign}(\mathbf{s}) \right). \end{aligned} \quad (53)$$

In controller 3, the SM surface and the control input are represented as

$$\mathbf{s} = \dot{\mathbf{e}} + \mathbf{c}_1 \mathbf{e}, \quad (54)$$

$$\begin{aligned} \tau = & \mathbf{M}(\mathbf{q})\ddot{\mathbf{q}}_d - \mathbf{M}(\mathbf{q})\mathbf{c}_1 \dot{\mathbf{e}} + \mathbf{M}(\mathbf{q}) \left( -\frac{\mathbf{k}_2}{\mathbf{F}(\mathbf{s})} |\mathbf{s}|^{b_2} \text{sign}(\mathbf{s}) - \mathbf{k}_3 \mathbf{s} \right. \\ & \left. - \left( \hat{\mathbf{v}}_1 + \hat{\mathbf{v}}_2 |\mathbf{q}| + \hat{\mathbf{v}}_3 |\dot{\mathbf{q}}|^2 \right) \text{sign}(\mathbf{s}) \right) + \mathbf{C}(\mathbf{q}, \dot{\mathbf{q}})\dot{\mathbf{q}} + \mathbf{G}(\mathbf{q}), \end{aligned} \quad (55)$$

where  $\mathbf{F}(s_i)_i = f_{3i} \text{arccot}(f_{2i} |s_i|^{f_{1i}})$ ,  $f_{3i} > \frac{2}{\pi}$ ,  $f_{2i} > 0$ , and  $0 < f_{1i} \leq 1$ .

In controller 4, the SM surface and the control input are represented as

$$\mathbf{s} = \dot{\mathbf{e}} + \mathbf{c}_1 \mathbf{e}, \quad (56)$$

$$\begin{aligned} \tau = & \mathbf{M}(\mathbf{q})\ddot{\mathbf{q}}_d - \mathbf{M}(\mathbf{q})\mathbf{c}_1 \dot{\mathbf{e}} \\ & + \mathbf{M}(\mathbf{q}) \left( -\mathbf{k}_1 |\mathbf{s}|^{b_1} \text{sign}(\mathbf{s}) - \mathbf{k}_2 |\mathbf{s}|^{b_2} \text{sign}(\mathbf{s}) \right. \\ & \left. - \left( \hat{\mathbf{v}}_1 + \hat{\mathbf{v}}_2 |\mathbf{q}| + \hat{\mathbf{v}}_3 |\dot{\mathbf{q}}|^2 \right) \text{sign}(\mathbf{s}) \right) \\ & + \mathbf{C}(\mathbf{q}, \dot{\mathbf{q}})\dot{\mathbf{q}} \\ & + \mathbf{G}(\mathbf{q}). \end{aligned} \quad (57)$$

According to the aforementioned analysis, it is clear that the SM surface designed in this paper is a further improvement of the SM surface corresponding to controller 2, while the reaching law corresponding to controller 1 developed in this paper has the adaptive capability. The SM surfaces corresponding to controllers 3 and 4 are special cases of the SM surface corresponding to controller 1. The above



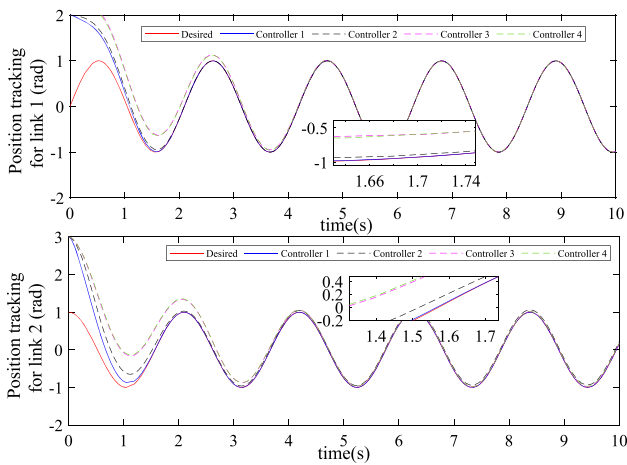


**Fig. 1** Trajectory tracking curve

four control schemes are compared to show the superiority of the controller developed in this paper. The above four controller parameters are roughly the same, and after the trial-and-error method of adjustment, the SM surface parameters are  $\mathbf{c}_1 = \mathbf{c}_2 = \mathbf{c}_3 = \text{diag}(1, 1)$ ,  $\mathbf{a}_1 = \text{diag}(9/5, 9/5)$ ,  $\mathbf{a}_2 = \text{diag}(5/9, 5/9)$ ,  $\mathbf{a}_3 = \text{diag}(1.8, 1.8)$ ,  $\mathbf{w}_1 = \text{diag}(0.4, 0.4)$ , and  $\boldsymbol{\mu} = \text{diag}(0.01, 0.01)$ . The reaching law parameters are  $\mathbf{k}_1 = \mathbf{k}_2 = \mathbf{k}_3 = \text{diag}(2, 2)$ ,  $\mathbf{b}_1 = \text{diag}(1.5, 1.5)$ ,  $\mathbf{b}_2 = \text{diag}(0.5, 0.5)$ ,  $\mathbf{h}_2 = \text{diag}(0.1, 0.1)$ ,  $\mathbf{h}_3 = \text{diag}(0.6, 0.6)$ , and  $\mathbf{h}_4 = \text{diag}(0.7, 0.7)$ . The adaptive law parameters are  $\mathbf{p}_1 = \mathbf{p}_2 = \mathbf{p}_3 = \text{diag}(0.008, 0.008)$  and  $\mathbf{m}_1 = \mathbf{m}_2 = \mathbf{m}_3 = \text{diag}(0.01, 0.01)$ . The two joints of the desired trajectory are  $\sin(3t)$  and  $\cos(3t)$ , respectively. The interference is unified as  $\boldsymbol{\tau}_d = \begin{bmatrix} 1 + 2 \sin(2\pi t) \\ 1 + 2 \sin(2\pi t) \end{bmatrix}$ .

**Case 1**

In the case of uniform parameter size, the simulation results are shown in Figs. 1, 2, 3, 4, 5 and 6.

Figures 1 and 2 show the tracking trajectory and error convergence curves, respectively. From the figures, it can be seen that the control scheme designed in this paper has the best tracking accuracy and speed under the condition of the same initial position error. From the enlarged view of Fig. 1, it can be seen that under the action of controller 1, the actual trajectory converges to the given trajectory with the least time and the fastest speed, followed by controller 2, and controllers 3 and 4 converge with little difference in speed. Analysis of the enlarged graph in Fig. 2 shows that the error fluctuation range is minimized with the best steady-state error under the control scheme presented in this work. The above analysis fully indicates the superiority of the nonsingular fixed-time SM surface and the enhanced reaching law presented in this work.

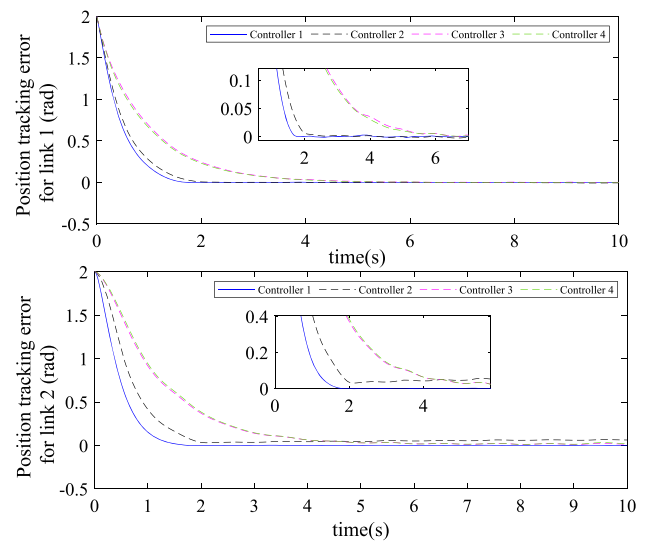


**Fig. 2** Error convergence curve

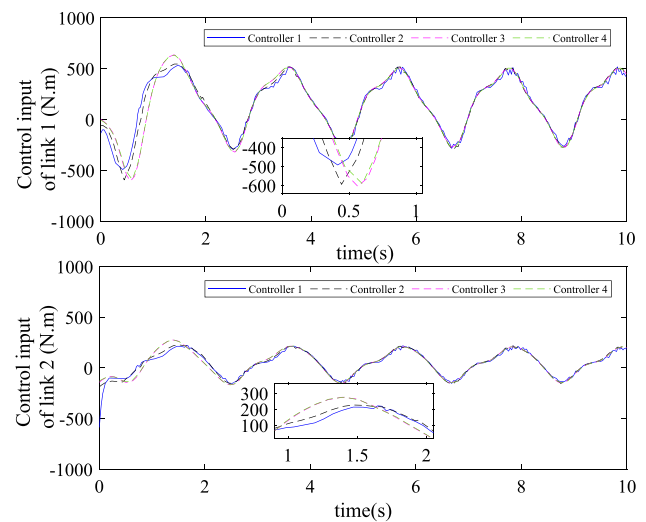


**Fig. 3** Control input curve

Analysis of Fig. 3 shows that the four controller amplitudes do not differ much, but the system state has the best comprehensive performance under the controller proposed in this paper, which further demonstrates the effectiveness of the control scheme in this work. It is worth mentioning that to make the system error quickly track the given trajectory, the initial torque will be larger under controller 1, which does not have a great influence on the actual performance considering the small time used. Figures 4, 5 and 6 demonstrate the interference upper bound estimation curve, which solves the prior knowledge of the interference by estimating the unknown interference upper bound coefficients. The introduction of adaptive law technology makes the system more conducive to the use of the actual system, making its controller more widely used.

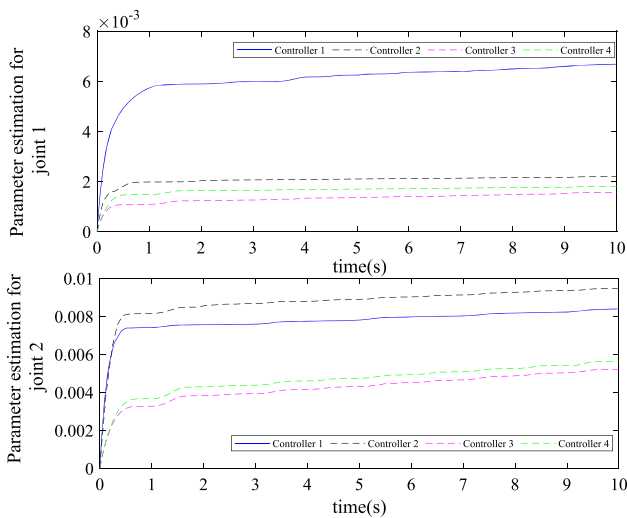


Fig. 4 Parameter  $v_1$  estimation curve

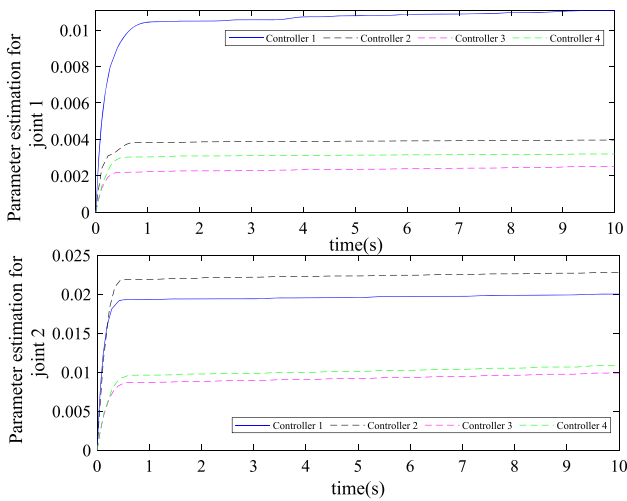


Fig. 5 Parameter  $v_2$  estimation curve

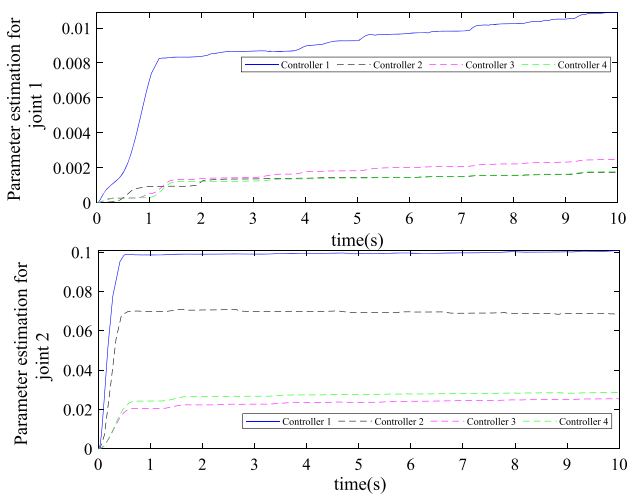


Fig. 6 Parameter  $v_3$  estimation curve

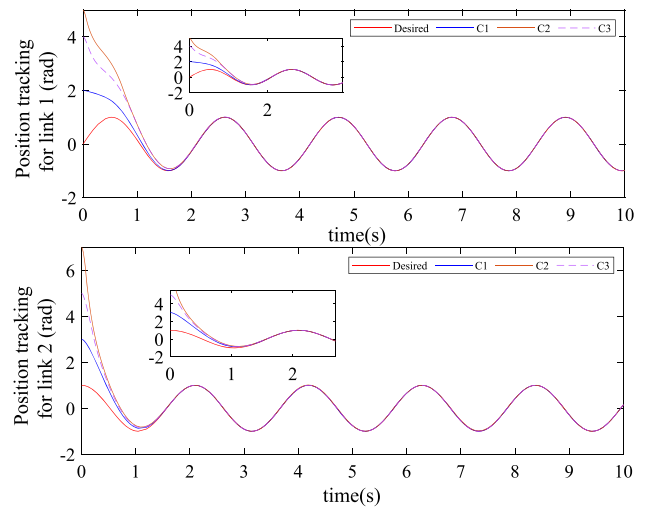


Fig. 7 Comparison of trajectory tracking with different initial errors

Considering that the upper bound of the fixed convergence time cannot actually be calculated, the initial position is adjusted to verify the fixed-time convergence characteristics of the controller. The simulation is performed separately for different initial positions under the action of controller 1, and the results are shown in Fig. 7. C1, C2, and C3 are different initial position sizes, respectively. Analysis of Fig. 7 and its enlargement shows that it is obvious that joints 1 and 2 track on the desired trajectory at 1.9 s and 1.5 s, respectively, with less dependence on the initial position size, which fully illustrates the effectiveness of the fixed-time controller and further proves the correctness of the analysis of the fixed-time characteristics of this paper.

### Case 2

Measurement noise is inevitable in the robotic manipulator system. Case 2 further considers the effect of measurement noise on the basis of Case 1 [37], and the results are displayed in Figs. 8, 9.

Analysis of Fig. 8 shows that the controller developed in this work still has the best error convergence rate and tracking accuracy with the effect of measurement noise. For the tracking error results, this paper uses the root-mean-square error (RMSE) and the average absolute error (AAE) for calculation, and both are expressed as

$$RMSE = \sqrt{\sum_{i=1}^X |e(i)|^2 / X}, \tag{58}$$

$$AAE = \sum_{i=1}^X |e(i)| / X. \tag{59}$$

For the tracking error brought into RMSE and AAE for calculation, the results are displayed in Table 1.

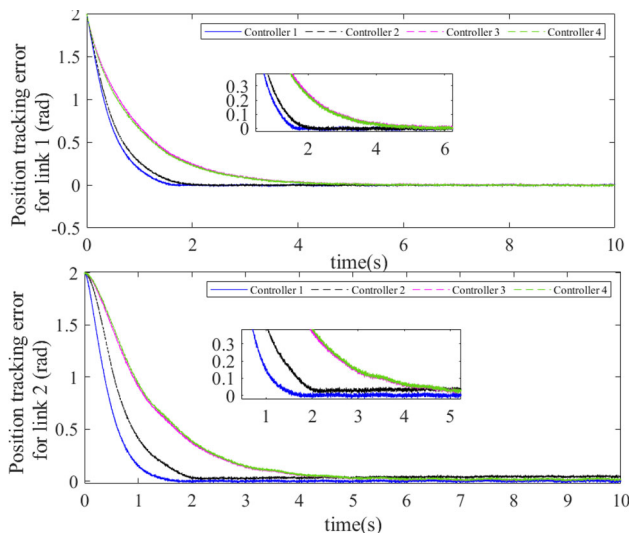


**Fig. 8** Error convergence curve

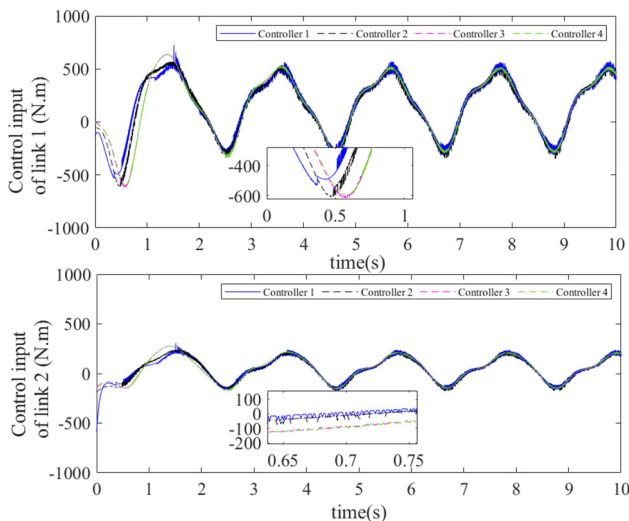


**Fig. 9** Control torque curve

**Table 1** Comparison of tracking error RMSE values and AAE values

(Degree)	RMSE (joint 1/2)	AAE (joint 1/2)
Proposed	0.2958/0.3214	0.1478/0.1574
Controller 2	0.3106/0.3801	0.1642/0.2124
Controller 3	0.3781/0.4642	0.2501/0.3216
Controller 4	0.3721/0.4711	0.2436/0.3284

Table 1 shows the final consequences of the RMSE and AAE comparisons for different controllers. With the proposed controller, joints 1 and 2 possess the smallest RMSE and AAE values, and this result shows the validity of the controller presented in this work. Figure 9 shows the torque curves of the different controllers under the effect of measurement noise. All four controllers possess a certain amount of

chatter, which is due to the impact of measurement noise and can be suppressed by filters [37].

## Conclusion

This paper proposes a new adaptive nonsingular fixed-time control method for robotic manipulator systems with disturbance uncertainty. By designing a novel SM surface and reaching law, the comprehensive performance in different stages is effectively improved. Second, for the case where the upper bound of the interference is unknown, this paper suppresses the effect of the disturbance on the system by estimating it through an adaptive technique. The stability of the closed-loop system is also analyzed, and it is demonstrated that the system state can reach the balance point at a fixed upper bound time. Finally, a simulation comparison with different control schemes reflects the effectiveness of the control method raised in this work and the small dependence of the convergence time on the initial conditions of the system. The control method designed in this work is also used in other nonlinear systems. Future work considers validating the control scheme of our method with a real robot system.

**Acknowledgements** This work is supported by the Natural Science Foundation of Gansu Province (20JR5RA419), Lanzhou Jiaotong University-Tianjin University Innovation Fund Project (2019053), and Gansu Provincial Department of Education: Innovation Fund Project of Gansu Provincial Higher Education (2022A-045).

## Declarations

**Conflict of interest** The author declared no potential conflicts of interest with respect to the research, authorship, and/or publication of this article.

**Open Access** This article is licensed under a Creative Commons Attribution 4.0 International License, which permits use, sharing, adaptation, distribution and reproduction in any medium or format, as long as you give appropriate credit to the original author(s) and the source, provide a link to the Creative Commons licence, and indicate if changes were made. The images or other third party material in this article are included in the article’s Creative Commons licence, unless indicated otherwise in a credit line to the material. If material is not included in the article’s Creative Commons licence and your intended use is not permitted by statutory regulation or exceeds the permitted use, you will need to obtain permission directly from the copyright holder. To view a copy of this licence, visit <http://creativecommons.org/licenses/by/4.0/>.

## References

- Zheng Z, Feroskhan M, Sun L (2018) Adaptive fixed-time trajectory tracking control of a stratospheric airship. *ISA Trans* 76:134–144

2. Ren C, Li X, Yang X, Ma S (2019) Extended state observer-based sliding mode control of an omnidirectional mobile robot with friction compensation. *IEEE Trans Ind Electron* 66(12):9480–9489
3. Xiao J, Zeng Z, Wu A, Wen S (2020) Fixed-time synchronization of delayed Cohen-Grossberg neural networks based on a novel sliding mode. *Neural Netw* 128:1–12
4. Xia H, Guo P (2022) Sliding mode-based online fault compensation control for modular reconfigurable robots through adaptive dynamic programming. *Complex Intell Syst* 8:1963–1973
5. Jiang Y, Zhang Y, Wang H, Liu K (2022) Sliding-mode observers based distributed consensus control for nonlinear multi-agent systems with disturbances. *Complex Intell Syst* 8:1889–1897
6. Ebrahimi Mollabashi H, Mazinan AH (2019) Incremental SMC-based CNF control strategy considering magnetic ball suspension and inverted pendulum systems through cuckoo search-genetic optimization algorithm. *Complex Intell Syst* 5(3):353–362
7. Sun H, Hou L, Li C (2019) Synchronization of single-degree-of-freedom oscillators via neural network based on fixed-time terminal sliding mode control scheme. *Neural Comput Appl* 31(10):6365–6372
8. Aouiti C, Jallouli H (2021) New feedback control techniques of quaternion fuzzy neural networks with time-varying delay. *Int J Robust Nonlinear Control* 31(7):2783–2809
9. Yang G, Wang H (2022) Neuroadaptive control of information-poor servomechanisms with smooth and nonsmooth uncertainties. *Complex Intell Syst* 8:2527–2539
10. Van M, Ge SS (2021) Adaptive fuzzy integral sliding-mode control for robust fault-tolerant control of robot manipulators with disturbance observer. *IEEE Trans Fuzzy Syst* 29(5):1284–1296
11. Van M (2021) Higher-order terminal sliding mode controller for fault accommodation of Lipschitz second-order nonlinear systems using fuzzy neural network. *Appl Soft Comput* 104:107186
12. Zhong Z, Wang X, Lam H-K (2021) Finite-time fuzzy sliding mode control for nonlinear descriptor systems. *IEEE/CAA J Autom Sin* 8(6):1141–1152
13. Teng L, Gull MA, Bai S (2020) PD-based fuzzy sliding mode control of a wheelchair exoskeleton robot. *IEEE/ASME Trans Mechatron* 25(5):2546–2555
14. Pazooki M, Mazinan AH (2018) Hybrid fuzzy-based sliding-mode control approach, optimized by genetic algorithm for quadrotor unmanned aerial vehicles. *Complex Intell Syst* 4(2):79–93
15. Long H, Guo T, Zhao J (2022) Adaptive disturbance observer based novel fixed-time nonsingular terminal sliding mode control for a class of DoF nonlinear systems. *IEEE Trans Industr Inf* 18(9):5905–5914
16. Huang Y, Jia Y (2019) Adaptive fixed-time six-DOF tracking control for noncooperative spacecraft fly-around mission. *IEEE Trans Control Syst Technol* 27(4):1796–1804
17. Kali Y, Saad M, Benjelloun K, Khairallah C (2018) Super-twisting algorithm with time delay estimation for uncertain robot manipulators. *Nonlinear Dyn* 93(2):557–569
18. Wang J, Zhao L, Yu L (2021) Adaptive terminal sliding mode control for magnetic levitation systems with enhanced disturbance compensation. *IEEE Trans Ind Electron* 68(1):756–766
19. Yang L, Yang J (2011) Nonsingular fast terminal sliding-mode control for nonlinear dynamical systems. *Int J Robust Nonlinear Control* 21(16):1865–1879
20. Ali N, Tawiah I, Zhang W (2020) Finite-time extended state observer based nonsingular fast terminal sliding mode control of autonomous underwater vehicles. *Ocean Eng* 218:108179
21. Zeng T, Ren X, Zhang Y (2020) Fixed-time sliding mode control and high-gain nonlinearity compensation for dual-motor driving system. *IEEE Trans Ind Inf* 16(6):4090–4098
22. Xu D, Ding B, Jiang B, Yang W, Shi P (2022) Nonsingular fast terminal sliding mode control for permanent magnet linear synchronous motor via high-order super-twisting observer. *IEEE/ASME Trans Mechatron* 27(3):1651–1659
23. Boukattaya M, Mezghani N, Damak T (2018) Adaptive nonsingular fast terminal sliding-mode control for the tracking problem of uncertain dynamical systems. *ISA Trans* 77:1–19
24. Wang Y, Zhu K, Chen B, Jin M (2020) Model-free continuous nonsingular fast terminal sliding mode control for cable-driven manipulators. *ISA Trans* 98:483–495
25. Wang Y, Li S, Wang D, Ju F, Chen B, Wu H (2021) Adaptive time-delay control for cable-driven manipulators with enhanced nonsingular fast terminal sliding mode. *IEEE Trans Ind Electron* 68(3):2356–2367
26. Polyakov A (2011) Nonlinear feedback design for fixed-time stabilization of linear control systems. *IEEE Trans Autom Control* 57(8):2106–2110
27. Ni J, Liu L, Liu C, Hu X, Li S (2017) Fast fixed-time nonsingular terminal sliding mode control and its application to chaos suppression in power system. *IEEE Trans Circ Syst II Express Briefs* 64(2):151–155
28. Chen Q, Xie S, He X (2021) Neural-network-based adaptive singularity-free fixed-time attitude tracking control for spacecrafts. *IEEE Trans Cybern* 51(10):5032–5045
29. Chen Q, Xie S, Sun M, He X (2018) Adaptive nonsingular fixed-time attitude stabilization of uncertain spacecraft. *IEEE Trans Aerosp Electron Syst* 54(6):2937–2950
30. Chen Q, Tao M, He X, Tao L (2021) Fuzzy adaptive nonsingular fixed-time attitude tracking control of quadrotor UAVs. *IEEE Trans Aerosp Electron Syst* 57(5):2864–2877
31. Zuo Z, Tie L (2014) A new class of finite-time nonlinear consensus protocols for multi-agent systems. *Int J Control* 87(2):363–370
32. Zuo Z (2015) Non-singular fixed-time terminal sliding mode control of non-linear systems. *IET Control Theory Appl* 9(4):545–552
33. Feng Y, Yu X, Man Z (2002) Non-singular terminal sliding mode control of rigid manipulators. *Automatica* 38(12):2159–2167
34. Zhang X, Xu W, Lu W (2021) Fractional-order iterative sliding mode control based on the neural network for manipulator. *Mathem Probl Eng* Vol.2021, Article ID 9996719, 12 pages
35. Chen Q, Yang C-B, Nan Y-R (2021) Disturbance rejection control of Buck converters based on variable rate reaching law. *Kongzhi yu Juece/Control Decis* 36(4):893–900
36. Li H, Cai Y (2016) Sliding mode control with double power reaching law. *Control Decis* 31(3):498–502
37. Wang Y, Gu L, Xu Y, Cao X (2016) Practical tracking control of robot manipulators with continuous fractional-order nonsingular terminal sliding mode. *IEEE Trans Ind Electron* 63(10):6194–6204

**Publisher's Note** Springer Nature remains neutral with regard to jurisdictional claims in published maps and institutional affiliations.